

# Electrical conduction mechanism in GeSeSb chalcogenide glasses

VANDANA KUMARI\*, ANUSAIYA KASWAN, D PATIDAR, KANANBALA SHARMA  
and N S SAXENA

Department of Physics, Semi-conductor & Polymer Science Laboratory, Room No. 14-15,  
University of Rajasthan, Jaipur 302 004, India

MS received 6 September 2014; accepted 7 September 2015

**Abstract.** Electrical conductivity of chalcogenide glassy system  $\text{Ge}_{30-x}\text{Se}_{70}\text{Sb}_x$  ( $x = 10, 15, 20$  and  $25$ ) prepared by melt quenching has been determined at different temperatures in bulk through the  $I$ - $V$  characteristic curves. It is quite evident from results that Poole–Frenkel conduction mechanisms hold good for conduction in these glasses in a given temperature range. The variation in electrical conductivity with composition was attributed to the Se–Sb bond concentration in the Se–Ge–Sb system. Results indicated that  $\text{Ge}_5\text{Se}_{70}\text{Sb}_{25}$  showed the minimum resistance. In view of this the composition  $\text{Ge}_5\text{Se}_{70}\text{Sb}_{25}$  may be coined as ‘critical composition’ in the proposed series. Also the activation energies of conduction of these glassy alloys have been calculated in higher and lower temperature range using the Arrhenius equation.

**Keywords.** DC conductivity; chalcogenide glass; Sb–Se bonding; Poole–Frenkel mechanism.

## 1. Introduction

To the best of our knowledge, every sector of scientific field, especially in material science, has gained remarkable improvements. Despite of several existing semiconducting materials (e.g., Si, Ge, GaAs and many more) and oxide semiconductors, the amorphous semiconductors or non-oxide glasses have also proved their utility at technological level due to variety of special optical, electrical, dielectrical and thermo-physical properties [1–3]. Chalcogenide glassy materials are applicable in various technologies owing to adequate amorphous semiconducting features [4,5].

It has been found that Se is of special interest, due to its device applications such as photocells, rectifier, xerography, etc [6]. Se in its pure form consists of mixed long polymeric  $\text{Se}_n$  chains along with ring fragments in various portions of chain which shows that the structure is a mixture of  $\text{Se}_n$  chains and  $\text{Se}_8$  rings [7]. On the addition of network formers or bond modifiers such as Ge, it is noted that  $\text{Ge}(\text{Se}_{1/2})_4$  tetrahedral units are formed [8]. Ge–Se chalcogenide glasses are very eco-friendly in comparison to arsenic-based glasses. When Sb is added to GeSe binary system, the glass-forming region increases, and compositional and configurational disorder takes place in the system. It has been observed that the addition of small quantity of Sb to Ge–Se glasses reduces the optical loss significantly [9].

Ge–Sb–Se chalcogenides are good candidates for the realization of opto-chemical sensors [10] which can be used in the rapid detection and identification of pollutant gases. Chalcogenides glasses also have solid-state technical importance as

some amorphous Se-binary alloys exhibit several anomalous features such as a negative Seebeck co-efficient [11], large Fermi level shift [12] and large photo-voltaic effect [13]. The  $I$ - $V$  characteristics of these glasses have been explained by many models such as Poole–Frenkel effect [14], tunnelling conduction [15], hopping conduction [16] and space charge limited conduction [17].

Efforts [18] have also been made by many workers from time to time to investigate the composition, temperature and field-effect dependence of the conductivity of the chalcogenide glasses because the results of such studies provide ways to control effectively the conductivity of amorphous semiconductors. The electrical transport properties of the material are of great importance in determining whether the material is congruent with our necessities or not. Therefore, it is worth to study the dependence of the electrical properties on composition as well as on temperature of  $\text{Ge}_{30-x}\text{Se}_{70}\text{Sb}_x$  ( $x = 10, 15, 20$  and  $25$ ) glasses.

## 2. Experimental

Four chalcogenide glasses from the  $\text{Ge}_{30-x}\text{Se}_{70}\text{Sb}_x$  system have been synthesized by the well-established melt quenching technique for conduction of the investigations. The compositions of these materials were taken as  $\text{Ge}_{30-x}\text{Se}_{70}\text{Sb}_x$  ( $x = 10, 15, 20$  and  $25$ ). High-purity (5 N pure) Ge, Se and Sb were kept in a quartz ampoule (internal diameter 12 mm) in appropriate atomic weight percentage according to the above-said compositions, they have evacuated and sealed. High vacuum ( $\sim 10^{-6}$  Torr) was created in the ampoules to avoid oxidation of materials at high temperature. Each ampoule was kept inside the furnace at  $925^\circ\text{C}$  (where

\* Author for correspondence (vandana.spsl@gmail.com)

the temperature of the furnace was raised at a rate of 3–4 °C min<sup>-1</sup>). The ampoules were rocked frequently for 12–14 h at the maximum temperature to make the melt homogeneous. Quenching of the melt was carried out in ice-cooled water to obtain glassy state.

The glasses, thus prepared, were ground to make fine powder for further studies. The glassy character of the powder of quenched ingots was confirmed by X-ray diffraction

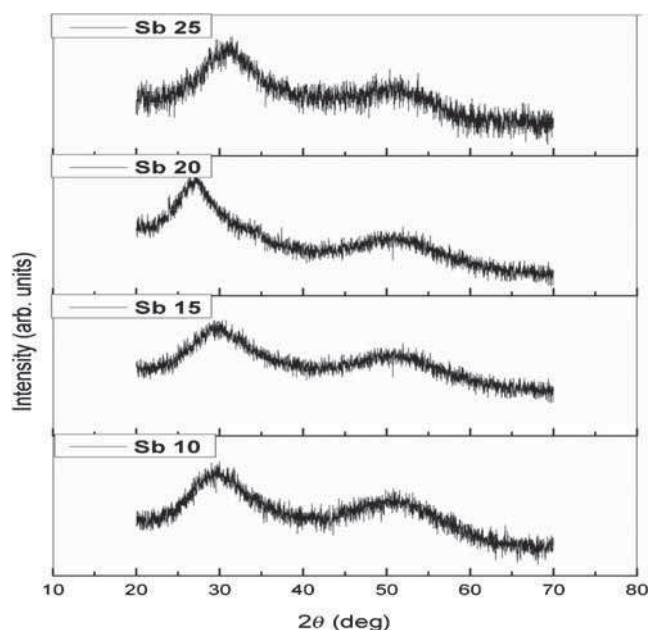


**Figure 1.** XRD patterns of  $\text{Ge}_{30-x}\text{Se}_{70}\text{Sb}_x$  ( $x = 10, 15, 20$  and  $25$ ) chalcogenide glasses.

(XRD) patterns using Bragg–Brentano geometry on Panalytical X'pert Pro Diffractometer with  $\text{Cu K}\alpha$  radiation source ( $\lambda = 1.5406 \text{ \AA}$ ). XRD patterns of  $\text{Ge}_{30-x}\text{Se}_{70}\text{Sb}_x$  ( $x = 10, 15, 20$  and  $25$ ) chalcogenide glasses are shown in figure 1. From the fine powder of glasses, the pellets, with diameter of 12 mm and thickness of 1 mm were prepared by applying a load of 5 ton. Studies of  $I$ – $V$  characteristics of  $\text{Ge}_{30-x}\text{Se}_{70}\text{Sb}_x$  ( $x = 10, 15, 20$  and  $25$ ) were performed on Keithley High Resistance Meter/Electrometer 6517A. These measurements were taken at room temperature as well as elevated temperatures in the range from room temperature to 200°C. This electrometer (6517A) has an in-built capability of output-independent voltage source of  $\pm 1000 \text{ V}$ . Hence, the same equipment (6517A) was used to apply the voltage (voltage range from 0 to 100 V) across the sample and to measure the current through the sample. To ensure the proper connection to the sample, the indigenously designed sample holder with copper electrodes was used. In this arrangement the sample was sandwiched between two circular electrodes of copper with the help of pressure contact arrangement.

### 3. Result and discussions

The typical  $I$ – $V$  characteristics of all the samples under test were recorded at room temperature as well as elevated temperatures (in the range from room temperature to 200°C) in order to investigate the temperature and composition dependence of the DC electrical conductivities of these samples. Figure 2 shows the  $I$ – $V$  characteristics of  $\text{GeSeSb}$  glassy system at room temperature. As a representative case figure 3 shows the  $I$ – $V$  characteristics of  $\text{Ge}_5\text{Se}_{70}\text{Sb}_{25}$  glassy pellet

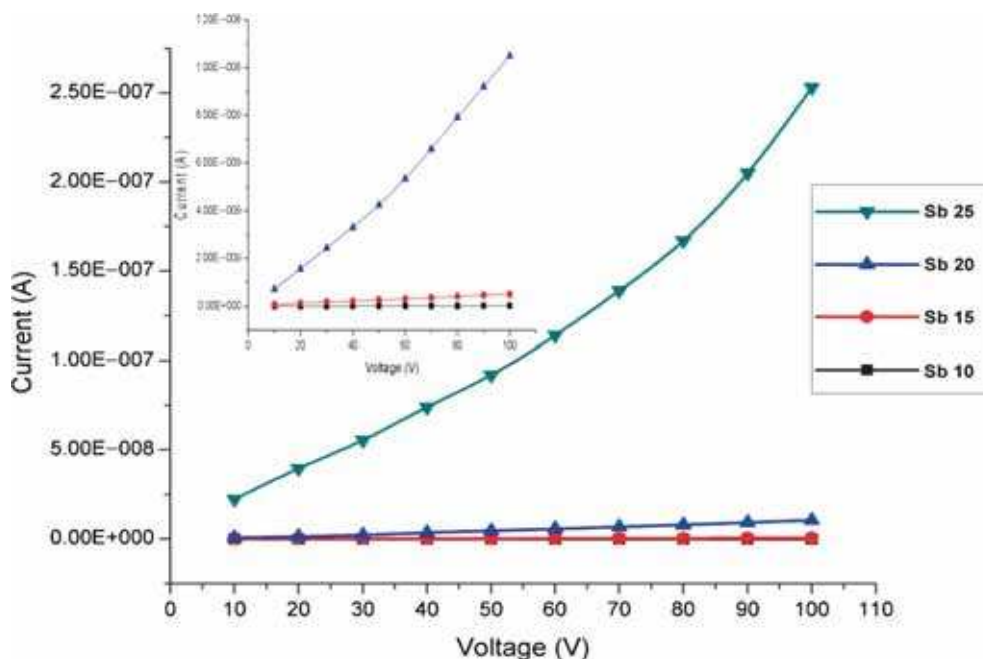


**Figure 2.**  $I$ – $V$  characteristics of  $\text{Ge}_{30-x}\text{Se}_{70}\text{Sb}_x$  ( $x = 10, 15, 20$  and  $25$ ) glasses at room temperature. (variation of current with voltage for  $x = 10, 15$  and  $20$  have been shown in the inset of the figure).

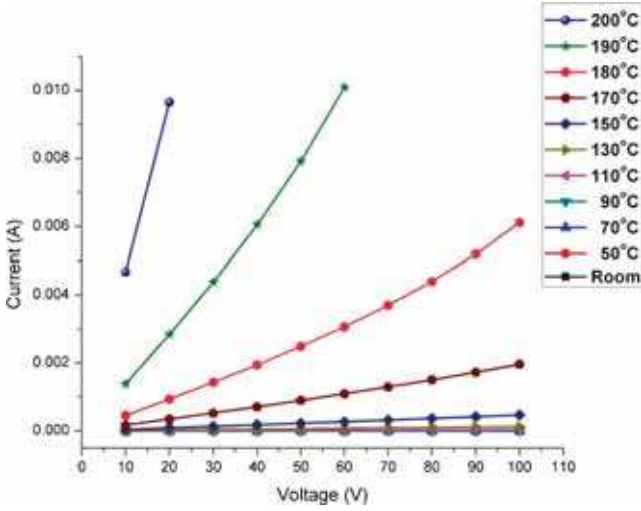


**Figure 3.**  $I$ - $V$  characteristics of  $\text{Ge}_5\text{Se}_{70}\text{Sb}_{25}$  glass at different temperatures as a representative case in the series.

at different temperatures. It is seen from figures 2 and 3 that  $I$ - $V$  characteristics of these samples have two linear regions. In low voltage range (from 0 to 50 V) both figures show the linear behaviour of the current. The  $I$ - $V$  characteristics depart from their behaviour ohmic to non-ohmic as the applied voltage across the sample increases.

The slope of linear regions gives us the values of resistance for that particular voltage range for different at% of Sb content. Table 1 shows the values of resistances for different voltage ranges. It has been observed that with increasing voltage across the sample, the resistance goes on decreasing slowly. It is evident from figure 2 that the resistance is lowest for the sample  $\text{Ge}_5\text{Se}_{70}\text{Sb}_{25}$ , i.e., it gives the maximum current among the compositions of the series under test at room temperature. Here one can infer that this composition has maximum conductivity as compared with other compositions of this series. The decreasing nature of resistance with respect to increasing temperature is the manifestation of the fact that the samples are showing the semiconducting nature with the increase of electrical conductivity.

In order to understand the electrical conduction through these materials completely, the problem is studied from two angles, i.e., composition dependence and temperature dependence of electrical conductivity. DC electrical conductivity is obtained from the relation

$$\sigma_{\text{DC}} = 1/\rho_{\text{DC}} = (1/R) (L/A), \quad (1)$$

where  $R$  is the resistance of the sample,  $L$  the thickness of the sample,  $A$  the cross-sectional area of the sample and  $\rho_{\text{DC}}$  the resistivity of the sample under test. It is well-established fact that the electrical conduction can be explained by means of two parallel mechanisms namely band conduction and hopping conduction. The band conduction occurs when the carriers are excited beyond the mobility edges into non-localized states at high temperatures. The excitations of the carriers

**Table 1.** Resistance of GeSeSb glass pellets (thickness 1 mm, diameter 12 mm) for two different ranges of applied potential difference.

| Composition                                  | Range                                  |   |
|--|--|---|
|  | $R_1 (\times 10^9 \Omega)$ for 10–50 V | $R_2 (\times 10^9 \Omega)$ for 60–100 V |
| $\text{Ge}_{20}\text{Se}_{70}\text{Sb}_{10}$ | 9.52                                   | 4.82                                    |
| $\text{Ge}_{15}\text{Se}_{70}\text{Sb}_{15}$ | 5.06                                   | 3.03                                    |
| $\text{Ge}_{10}\text{Se}_{70}\text{Sb}_{20}$ | 3.23                                   | 1.79                                    |
| $\text{Ge}_5\text{Se}_{70}\text{Sb}_{25}$    | 2.05                                   | 1.44                                    |

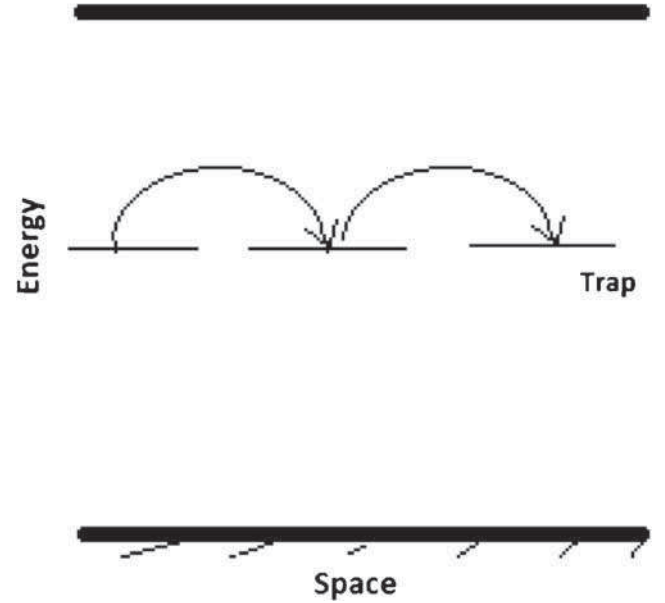


**Figure 4.** Schematic diagram for hopping conduction mechanism.

into localized states at band edges cause the hopping conduction [19]. It is known that unsaturated bonds are produced as a result of insufficient number of atoms in the amorphous material [20]. Semiconductors as Ge, Si are four-fold coordinated in crystalline materials. However in amorphous structure not all the atoms are four-fold coordinated due to continuous random network. Due to this disordered nature of amorphous materials some atoms feature an unsaturated bond (dangling bond (DB)). As discussed Se is two-fold coordinated having mainly chains and any chain end will be the site of unsaturated (dangling) bond. These DB can be described as broken covalent bonds. Therefore, in amorphous material due to the lack of ideal four-fold or two-fold symmetry unsaturated bonds generate.

Hopping is a current conduction mechanism in which charge carriers are ‘hopping’ from trap to trap. In hopping charges occasionally jump from trap to trap as shown in figure 4. The states in the tails of the conduction band and valance band of an amorphous semiconductor are localized. Electrons move among these states by ‘hopping’ from full states to empty states.

Thus, the total conductivity is given as

$$\sigma = \sigma_i + \sigma_h, \quad (2)$$

where  $\sigma_i$  is the intrinsic conductivity and  $\sigma_h$  the hopping conductivity.

It has been indicated [21] that in the glasses containing Se, there is a tendency to form polymerized network and homopolar bond is qualitatively suppressed. According to the Phillips model [22] of medium range order, germanium chalcogenides can be described as small chemically ordered clusters embedded in a continuous network.  $\text{Se}_n$  chains, corner-sharing tetrahedral  $\text{GeS}_2$  and the ethane like  $\text{GeSe}_3$  structural units are the building blocks of the  $\text{Ge}_x\text{Se}_{1-x}$  alloys. Feltz *et al* [23] concluded from radial distribution function studies, obtained from XRD measurements, that a large number of  $\text{GeSe}_2$  units are present in a three-dimensionally connected network of  $\text{Ge}_x\text{Se}_{1-x}$ . The addition of antimony to GeSe chalcogenides leads to a considerable reconstruction of the glass structure because of the change in the structural units that form a continuous network. Here Sb enters in the system at the cost of Ge and makes bonding with Se. It is also reported that the role of Ge on the formation of a three-dimensional network, through the apparition of  $\text{GeSe}_4$  and  $\text{GeSe}_2$  units at the expense of  $\text{SbSe}_3$  and  $\text{Se}_8$  groups, is evidenced, due a higher tendency of Ge to spontaneously form linkages with the other elements of the medium [24]. Therefore network linkage decreases with the increase in percentage of antimony and system tends to more relaxed structure. The bond energy of Sb–Se bonds is lower than the bond energy of Ge–Se bonds, and, the Sb–Sb bond is the weakest of the other bonds. These results support the view that the addition of Sb at the expense of Ge content makes the weak bonds with Se and relaxes the structure.

It is also reported by Haisty and Krebs [25] that the addition of a few percentages of Sb is sufficient to cause crystallization of Se unless some Ge is also present, in which case glasses are formed. In fact, 5% Ge is sufficient to ensure glass formation with upto about 30% Sb. This is because Ge is capable to form covalent bonds with Se atoms and connects chains mutually to form a strong three-dimensional network structure [26]. The role of Sb in promoting crystallization of Se was explained [25] in connection with Sb–Se system. It is mainly owing to the fact that Sb as a heavy element forms three weaker bonds in addition to the three strong bonds. Haisty *et al* [25] have given the schematic diagram (figure 5) to show that how Sb atom makes 3 weak bonds. Figure 5 shows the schematic representation of a possible mechanism by which Sb atom can disrupt neighbouring Se chains, by forming additional weak bonds. These weaker bonding forces have to direct themselves towards the Se atoms of the neighbouring chains or rings and thereby weaken the Se–Se bonds of these chains. Also, it is due to the fact that the Sb–Sb bond is weaker than the Se–Se bond. These effects are manifested in a higher conductivity in Sb–Se systems than in pure Se. Also in the present studied system, it is reported [27] that crystallization increases with the increase in concentration of Sb content.

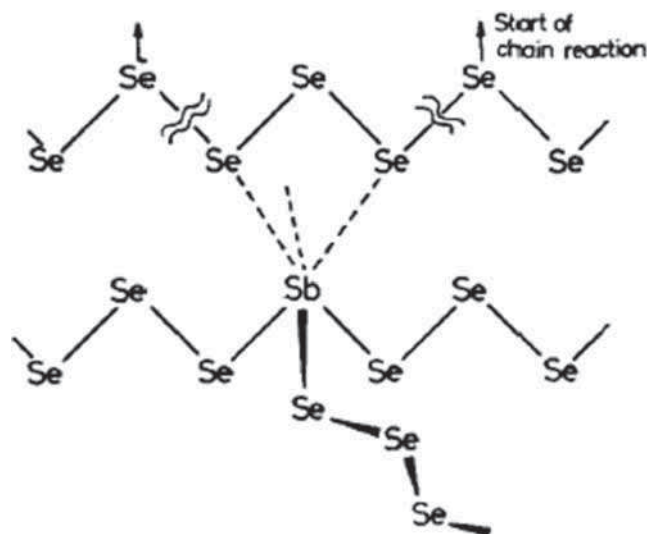


**Figure 5.** Schematic representation of a possible mechanism by which Sb atom can disrupt neighbouring Se chains, by forming additional weak bonds.

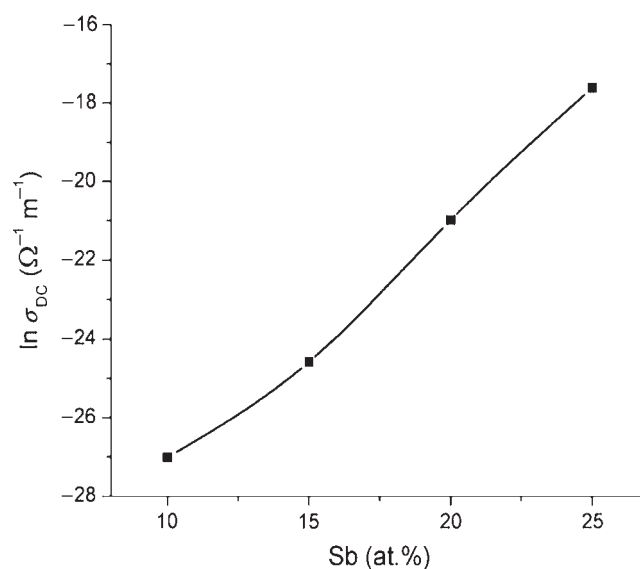


**Figure 6.** Composition dependence of conductivity of  $\text{Ge}_{30-x}\text{Sb}_x\text{Se}_{70}$  ( $x = 10, 15, 20$  and  $25$ ) glassy system at room temperature.

Thus, the addition of Sb increases the weak bond density in the system while Ge atoms form covalent bonds with Se atoms. Hence, it is reasonable to think that the increase of Sb content in the investigated system at the expense of Ge content decreases the covalent bond density and increases the weak bond density. In connection with the above-mentioned bonding and crystallization effects of Sb on Se, the decrease of covalent bond density and the increase of weak bond density results in higher conductivity. Figure 6 shows the composition dependence of conductivity for Ge–Se–Sb glassy system at room temperature. Here it is clear that the glass containing 25 at% of Sb can be considered as a critical

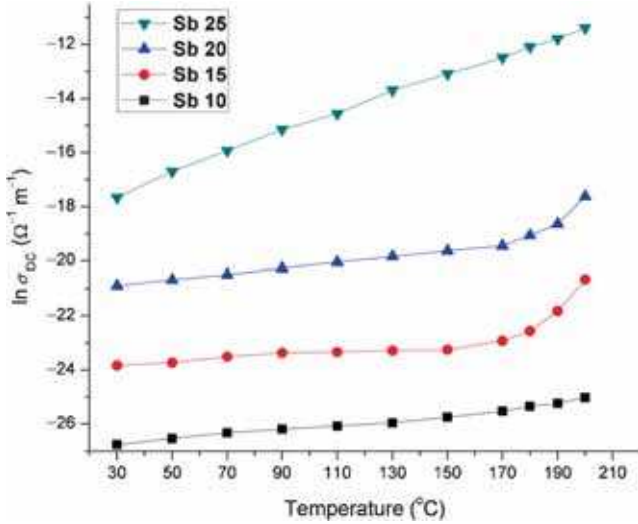


**Figure 7.** Temperature dependence of the conductivity of  $\text{Ge}_{30-x}\text{Se}_{70}\text{Sb}_x$  ( $x = 10, 15, 20$  and  $25$ ) glassy system.

composition at which the system has the maximum density of Sb–Se bonds in the series under study. Thus, the observed increase in electrical conductivity with the increase in Sb content (figure 6) may be because of the crystallization due to the decrease of covalent bond density and the increase of weak bond density.

In addition to this contributory factor of weak bond density, the effect of temperature and induced thermal effects due to higher voltage also contribute to the electrical conduction in such materials. Discussion can be initiated here with dividing the effects as (i) temperature effects and (ii) induced thermal effects at higher voltages.

In temperature effects it is clear that the conductivity of these samples increases with the increase in temperature which illustrates that these samples are semiconducting in nature. Figure 7 shows the temperature dependence of the conductivity of different samples. Composition having 25 at% of Sb allows the maximum current flow at all temperature that is clear from figure 7. The composition  $\text{Ge}_5\text{Se}_{70}\text{Sb}_{25}$  shows maximum DC electrical conductivity at all temperatures in bulk form. Keeping this in mind, the composition  $\text{Ge}_5\text{Se}_{70}\text{Sb}_{25}$  may be coined as ‘critical composition’.

In applied voltage effects when the increase of the voltage across the sample was continued, the induced thermal effects are produced at the higher voltage. These thermal effects allow more current to flow through the sample by decreasing its resistance and are responsible for the changing behaviour of  $I$ – $V$  characteristics in the higher voltage region from ohmic to non-ohmic.

The relation between the current and the square root of the applied voltage as given by Jonscher and Hill [28] is

$$I = I_{\text{PF}} \exp(\beta V^{1/2}/k_{\text{B}}T), \quad (3)$$

where

$$\beta = (e^3/4\pi\epsilon\epsilon_0d)^{1/2}, \quad (4)$$

$\epsilon_0$  is the permittivity of the space,  $\epsilon$  the relative permittivity of the sample,  $d$  the interspacing between filled and empty sites (jump distance), and  $I_{\text{PF}}$  (at  $V = 0$ ) is given by

$$I_{\text{PF}} = I_0 \exp(-\Phi/k_{\text{B}}T), \quad (5)$$

where  $\Phi$  is the trap depth and

$$I_0 = Anev. \quad (6)$$

In equation (6),  $A$  is the electrode area,  $n$  the carrier concentration,  $e$  the electronic charge and  $v$  is the phonon frequency ( $\approx 10^{13} \text{ s}^{-1}$ ) taken as constant [16].

According to equation (3) the linear relation between  $\ln(I)$  and  $V^{1/2}$  have been obtained for voltage ranges 10–50 and 60–100 V, respectively. However, a non-linearity (as shown in figures 8 and 9) is obtained when the relation is plotted for complete range of voltage from 10 to 100 V. Figure 9 shows the plot between  $\ln(I)$  and  $V^{1/2}$  for  $\text{Ge}_5\text{Se}_{70}\text{Sb}_{25}$  glass sample as representative case at different temperatures in this proposed study. Linearity of  $\ln(I)$  vs.  $V^{1/2}$  curve in figures 8 and 9 in the two voltage ranges suggests that the conduction in such materials obey the Poole–Frenkel conduction mechanism [29]. The linearity could be due to the absence of space charge resulting in a uniformity of field distribution between electrodes. The current in case of Poole–Frenkel effect remains unchanged when polarities of the electrodes are reversed. This is due to the fact that current does not depend upon the potential barrier at the interface. The Poole–Frenkel conduction mechanism deals with the conduction in such materials where defect/impurity generated traps are involved. Traps are additional energy states close to the band edge caused by the structural defects in the material or an impurity or charged point defect in semiconductor in which minority carrier can be trapped (captured) for a period of time and then released (thermally ‘ejected’) into the band from which it originated. These traps can trap the electrons and trapped electrons can escape by thermal emission; current flows due to electrons ‘jumping’ from trap to trap in the presence of electric field. These traps restrict the current flow because of a capture and emission process, thereby becoming the dominant current mechanism [30].

The variation of electrical conductivity with the reciprocal temperature in the temperature range from room temperature to 533 K for the system under study is displayed in figure 10 for different Sb concentrations. Figure 10 shows the plot of  $\ln(\sigma)$  vs.  $1/T$  for  $\text{Ge}_{30-x}\text{Se}_{70}\text{Sb}_x$  ( $x = 10, 15, 20$  and  $25$ ) glassy system and two linear regions in this plot were obtained. The non-linearity or sharp increase in conductivity between the temperature range 433–533 K indicates that there is an effect of thermodynamic transition (from glassy to crystalline or more ordered state) in the vicinity of a particular temperature which may be regarded as glass transition temperature and it is also supported by differential scanning calorimetry (DSC) thermogram of the samples reported earlier [27]. As the temperature increases beyond 433 K, i.e., glass transition range, nucleation and growth process start and glassy system leads to crystallization. With the growth

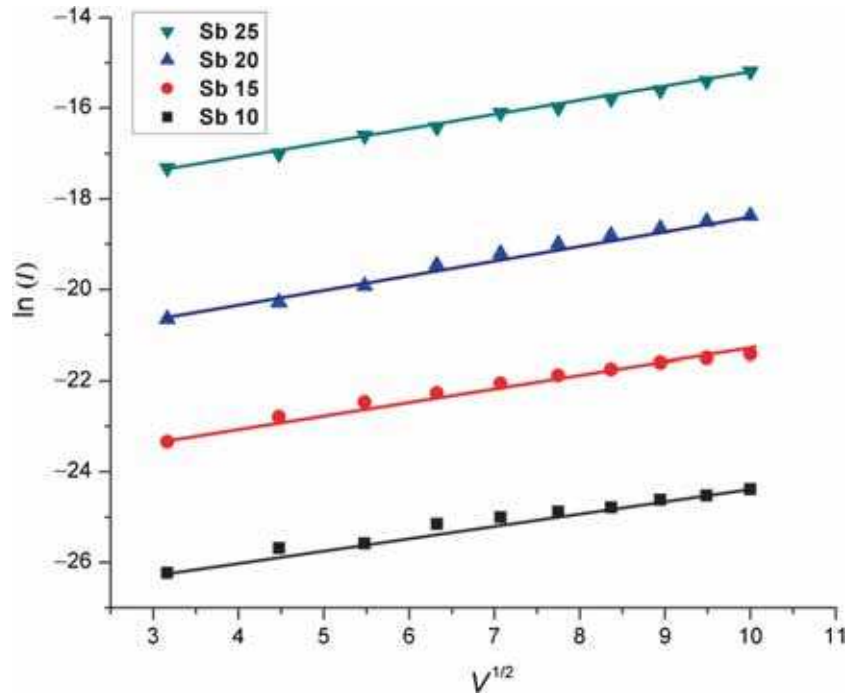


**Figure 8.** Linear relationship between  $\ln(I)$  and  $V^{1/2}$ : verification of Poole–Frenkel conduction mechanism of  $\text{Ge}_{30-x}\text{Se}_{70}\text{Sb}_x$  ( $x = 10, 15, 20$  and  $25$ ) glassy system at room temperature.

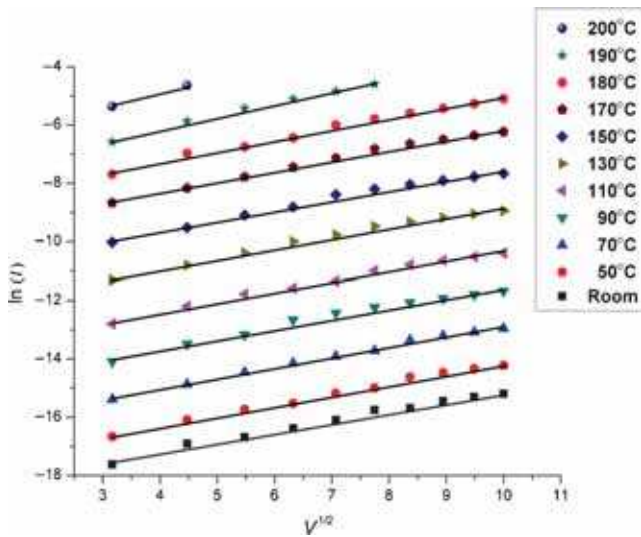


**Figure 9.** Verification of Poole–Frenkel conduction mechanism for  $\text{Ge}_5\text{Se}_{70}\text{Sb}_{25}$  glassy pellet as a representative case at different temperatures.

of the grains, the size of the grain increases with narrowing down to grain boundaries which in turn affect the conduction process. This is due to the fact that the available charge carriers will get the easier path to cross the grain boundaries, which is effectively responsible for the increment of current and hence conductivity in the temperature range beyond 433 K. Also this decrease in the resistance in this temperature range is caused due to the fact that glass is acquiring a more ordered state during crystallization. Figure 10 shows break

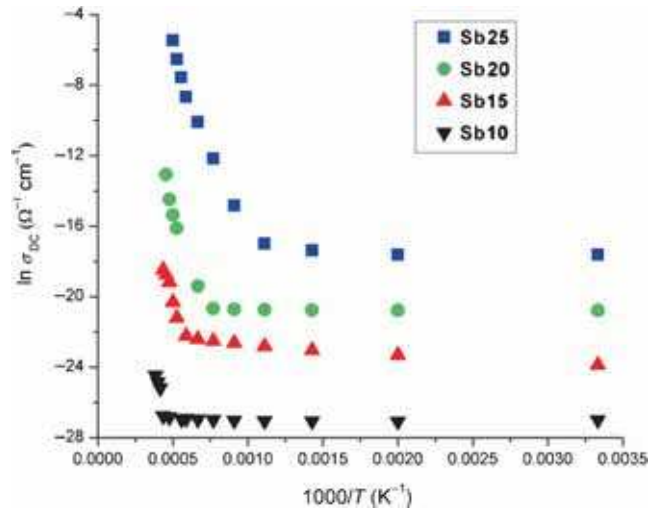


**Figure 10.** Variation in  $\ln \sigma_{DC}$  as a function of  $1/T$  for  $\text{Ge}_{30-x}\text{Se}_{70}\text{Sb}_x$  ( $x = 10, 15, 20$  and  $25$ ) glassy system.

in continuity of each curve and their kinks illustrate two different values of activation energy for each sample in higher and lower temperature range. For all samples, the electrical conductivity was found to be a negative exponential function of the absolute temperature according to the following Arrhenius relation [31]:

$$\sigma = \sigma_0 \exp(-\Delta E_c/k_B T), \quad (7)$$

where  $\sigma_0$  is the pre-exponential factor including charge carrier mobility and density of states,  $k_B$  is Boltzmann's

**Table 2.** Electrical parameters in GeSeSb glassy system at higher and lower temperature ranges.

| Sample   | In higher temperature range |   | In lower temperature range |   |
|--|-----------------------------|---|----------------------------|---|
|  | $\Delta E_{c1}$ (eV)        | $\sigma_{01}$ ( $\Omega^{-1}\text{cm}^{-1}$ ) | $\Delta E_{c2}$ (eV)       | $\sigma_{02}$ ( $\Omega^{-1}\text{cm}^{-1}$ ) |
| Ge <sub>20</sub> Se <sub>70</sub> Sb <sub>10</sub> | 1.18                        | $4.00 \times 10^{-11}$                        | 0.01                       | $2.59 \times 10^{-12}$                        |
| Ge <sub>15</sub> Se <sub>70</sub> Sb <sub>15</sub> | 1.3                         | $2.57 \times 10^{-8}$                         | 0.13                       | $6.9 \times 10^{-9}$                          |
| Ge <sub>10</sub> Se <sub>70</sub> Sb <sub>20</sub> | 1.40                        | $2.80 \times 10^{-7}$                         | 0.01                       | $1.4 \times 10^{-9}$                          |
| Ge <sub>5</sub> Se <sub>70</sub> Sb <sub>25</sub>  | 1.54                        | $4.93 \times 10^{-4}$                         | 0.09                       | $9.02 \times 10^{-7}$                         |

constant,  $T$  the absolute temperature and  $\Delta E_c$  the activation energy for conduction. Equation (7) may be written as

$$\ln \sigma_{DC} = \ln \sigma_0 - (\Delta E_c / k_B T) \quad (8)$$

or

$$\ln \sigma_{DC} = -(\Delta E_c / 1000 k_B) (1000 / T) + \ln \sigma_0. \quad (9)$$

When a graph is plotted between  $\ln \sigma_{DC}$  and  $1000/T$ , a straight line is obtained having slope  $(\Delta E_c / 1000 k_B)$  and intercept  $\ln \sigma_0$ . From the values of the slope and intercept activation energy and pre-exponential factor are calculated as follows:

$$\Delta E_c = 1000 \times k_B \times \text{slope of straight line,}$$

$$\sigma_0 = \sigma_{DC} / \exp(-\Delta E_c / k_B T).$$

The calculated values of activation energies ( $\Delta E_c$ ) and pre-exponential factors in the higher and lower temperature ranges, for each sample, are given in table 2. The values of activation energy in the low temperature range have lower values as compared to the values in the higher temperature range.

It is clear from table 2 that activation energy does not depend upon composition of glassy alloys in low temperature region. Therefore, the conduction in low temperature range may be less affected by Sb concentration. On the other hand activation energy is higher in higher temperature range and increases with the increase in Sb content for all the compositions of the system under investigations.

#### 4. Conclusions

The variation of  $I$ - $V$  characteristics and conductivities of Ge<sub>30-x</sub>Se<sub>70</sub>Sb<sub>x</sub> ( $x = 10, 15, 20$  and  $25$ ) have been discussed with composition and temperature. The conduction mechanism is explained in terms of the parent structure related to Se-Ge system, in addition to Sb inclusion, and in terms of Poole-Frenkel conduction mechanism. More precisely it can be concluded that

1. XRD results for the Ge<sub>30-x</sub>Se<sub>70</sub>Sb<sub>x</sub> ( $x = 10, 15, 20$  and  $25$ ) chalcogenide glasses in powder form have an amorphous structure.
2. The composition vs. conductivity plots are suggestive of the fact that composition Ge<sub>5</sub>Se<sub>70</sub>Sb<sub>25</sub> allows

maximum current to flow or in other words is most conductive in series. This composition will be useful for electrical applications bearing more temperatures (to be degraded) as compared with other members of the series.

3. Ge<sub>30-x</sub>Se<sub>70</sub>Sb<sub>x</sub> glassy materials do not follow the power law  $I = kV^m$ , where  $k$  and  $m$  are the constants, which is indicated by the slight non-linearity of  $I$ - $V$  characteristics of these samples. This variable rate of increasing current is an evidence for: (a) the increment in current with increasing applied voltage at a constant temperature, and (b) the increment in current with the increment in temperature at a constant voltage. These results ascertain the semiconducting nature of these samples. Here the conduction mechanism is assumed qualitatively in terms of Poole-Frenkel effect. Also the linear relation between  $\ln(I)$  and  $V^{1/2}$  approves the type of conduction mechanism as Poole-Frenkel.
4. The activation energy of conduction of these glassy alloys has been calculated using the Arrhenius equation in higher and lower temperature ranges. In low temperature range activation energy is almost independent of Sb concentration but in high temperature range the activation energy increases with the increase in Sb content for all the compositions.

#### Acknowledgements

Vandana Kumari is thankful to Council of Scientific and Industrial Research (CSIR), New Delhi (India), for providing research scholarship. We are also thankful to Dr Mahesh Baboo for his help in various ways during the course of this work.

#### References

- [1] Pamukchieva V, Szekeres A, Todorova K, Svab E and Fabian M 2009 *Opt. Mater.* **32** 45
- [2] Sharma J and Kumar S 2010 *J. Alloys Compd.* **506** 710
- [3] Gunti S R and Asokan S 2010 *J. Non-Cryst. Solids* **356** 1637
- [4] Singh A K 2012 *J. Non-oxide Glasses* **3** 1
- [5] Sharma N, Shukla S, Sharma J and Kumar S 2011 *J. Non-oxide Glasses* **3** 121
- [6] Ambika and Barman P B 2010 *Physica B* **405** 822

- [7] Sharma V 2006 *J. Phys.: Condens. Matter* **18** 10279
- [8] Sharma N, Sharda S, Sharma V and Sharma P 2011 *Defect Diffus. Forum* **316–317** 37
- [9] Ganjoo A, Jain H, Khalid S and Pantano C G 2005 *J. Philos. Mag. Lett.* **85** 503
- [10] Le Coq D, Boussard-Plédel C, Fonteneau G, Pain T, Bureau B and Adam J L 2003 *Mater. Res.* **38** 1745
- [11] Watanabe I and Yamamoto T 1985 *Jpn. J. Appl. Phys.* **24** 1282
- [12] Watanabe I and Sekiya T 1987 *J. Non-Cryst. Solids* **97–98** 667
- [13] Nang T T, Matsushita T, Okuda M and Suzuki A 1977 *Jpn. J. Appl. Phys.* **16** 253
- [14] Hill R M 1971 *Philos. Mag.* **23** 59
- [15] Stubb T, Suntla T and Tiainen O J A 1972 *Solid State Electron* **15** 611
- [16] Bagley B G 1970 *Solid State Commun.* **8** 345
- [17] Lampert M A and Mark P 1970 *Current injection in solids* (New York (NY): Academic Press) Part I, p 72 (Chapter 4)
- [18] El-Kady Y L A 1999 *Phys. Status Solidi (a)* **175** 577
- [19] Theye M L 1973 *Proceedings of the fifth international conference on amorphous and liquid semiconductors (Gramisch-Partenkirchen, Germany)* vol 1 p 479
- [20] Mott N F and Davis E A 1971 *Electronic processes in non-crystalline materials* (Oxford: Clarendon Press)
- [21] Rabinal M K, Ramesh Rao N, Sangunni K S and Gopal E S R 1994 *Philos. Mag. Part B* **70** 89
- [22] Phillips J C 1981 *J. Non-Cryst. Solids* **43** 37
- [23] Feltz A, Phole M, Steil H and Herms G 1985 *J. Non-Cryst. Solids* **69** 271
- [24] Sharma S, Sharma N, Sharma P and Sharma V 2013 *J. Non-Cryst. Solids* **362** 136
- [25] Haisty R W and Krebs H 1969 *J. Non-Cryst. Solids* **1** 399
- [26] Sakai H, Shimakawa K, Inagaki Y and Arizumi T 1974 *Jpn. J. Appl. Phys.* **13** 500
- [27] Kaswan A, Kumari V, Patidar D, Saxena N S and Sharma K 2014 *Process. Appl. Ceram.* **8** 25
- [28] Jonschere A K, Hill R M, Hass G M H and Hofman R W 1975 *Physics of thin films* (New York: Academic Press)
- [29] Abdel-Latif R M 1998 *Physica B* **254** 273
- [30] Saraswat V K, Singh K, Saxena N S, Kishore V, Sharma T P and Saraswat P K 2006 *Curr. Appl. Phys.* **6** 14
- [31] Davis E A and Mott N F 1970 *Philos. Mag.* **22** 903